

Gradient-based Class Weighting for Unsupervised Domain Adaptation in Dense Prediction Visual Tasks

Roberto Alcover-Couso¹, Marcos Escudero-Viñolo¹, Juan C. SanMiguel¹, and Jesus Bescos¹

Universidad Autonoma de Madrid

Abstract. In unsupervised domain adaptation (UDA), where models are trained on source data (e.g., synthetic) and adapted to target data (e.g., real-world) without target annotations, addressing the challenge of significant class imbalance remains an open issue. Despite considerable progress in bridging the domain gap, existing methods often experience performance degradation when confronted with highly imbalanced dense prediction visual tasks like semantic and panoptic segmentation. This discrepancy becomes especially pronounced due to the lack of equivalent priors between the source and target domains, turning class imbalanced techniques used for other areas (e.g., image classification) ineffective in UDA scenarios. This paper proposes a class-imbalance mitigation strategy that incorporates class-weights into the UDA learning losses, but with the novelty of estimating these weights dynamically through the loss gradient, defining a Gradient-based class weighting (GBW) learning. GBW naturally increases the contribution of classes whose learning is hindered by large-represented classes, and has the advantage of being able to automatically and quickly adapt to the iteration training outcomes, avoiding explicitly curricular learning patterns common in loss-weighting strategies. Extensive experimentation validates the effectiveness of GBW across architectures (convolutional and transformer), UDA strategies (adversarial, self-training and entropy minimization), tasks (semantic and panoptic segmentation), and datasets (GTA and Synthia). Analysing the source of advantage, GBW consistently increases the recall of low represented classes.

Keywords: Unsupervised Domain Adaptation · Class Imbalance · Semantic segmentation

1 Introduction

Dense prediction visual tasks entail a major challenge for the annotation of the required training datasets, as the annotation of a single image for semantic or panoptic segmentation is estimated to take more than an hour for an average

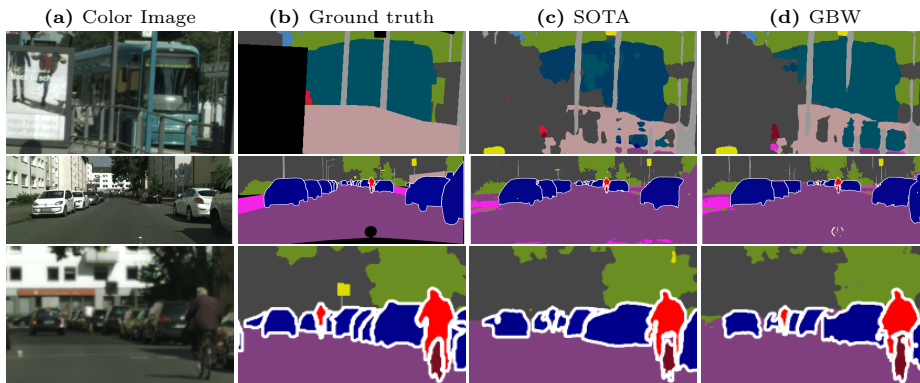


Fig. 1: UDA driven by MIC [18] (1st row) and EDAPS [34] (2nd and 3rd rows) methods is biased toward more populated (frequent or larger) classes on the source dataset (c), miss-classifying instances of less frequent or smaller classes: false positives examples include instances of *train*, *car* and *person* miss-classified as *truck*, *road* and *car* respectively. (d) GBW improves the classification of under-represented classes.

human [8, 12]. A bypass solution has been the use of synthetic datasets, as simulated environments can significantly reduce annotation costs. However, a network trained on a synthetic source dataset is expected to underperform when applied to the real target dataset, due to the data distribution co-variate shifts between domains. To mitigate this domain gap, unsupervised domain adaptation (UDA) is defined as the training of a deep learning model focused on generalizing to unlabeled target domains by leveraging labeled data from a source domain [16, 34, 43, 47].

UDA methods have remarkably progressed in the last few years and they still are a more effective solution for specific domains than foundational models [5] mainly due to their domain specificity. However, there is still a noticeable performance gap compared to supervised learning [2, 52, 57]. One of the factors contributing to this gap is the complexity of handling class imbalance. As an inherent factor of the data distribution, class imbalance is also subjected to covariant shifts and changes between the source and target domains. Strategies to handle class imbalance can be roughly divided into [20, 41]: data-level and algorithmic-level techniques. **Data-level** techniques [16–18, 34] can not cope with class-imbalance in dense visual tasks, as they cannot yield uniform class samplings due to the imbalance nature of these tasks, where context is key for prediction and the context of low populated classes is prone to be composed of large populated classes. Therefore, sampling *more* from the low populated classes entails including (eventually more) samples from large populated ones, keeping or even enlarging the imbalance. **Algorithmic-level** techniques assign different weights to the loss of different classes according to the target class distribution generally under a class-weighting strategy [20]. Class-weighting has the effect of differently pondering the contribution to the global training loss of the different classes [22]. Class-weighting techniques have been proven ineffec-

tive for UDA due to the lack of target domain class-frequencies [54, 55] and the discredited assumption that target domain class-frequency is equivalent to that of source domain [54, 55]. Therefore, the only feasible alternative is to estimate the target priors on every model update using pseudo-labels [54, 55], incurring excessive computational costs, and demotivating the use of algorithmic-level techniques [22].

UDA methods for image-classification have reported the advantages of assigning different relevance to the training samples through importance weighting [53]. Importance weighting prioritizes data points with high impact on the learning process by focusing on data that generates large gradients during optimization [21]. Adaptive weighting incorporates importance weighting in the training process by giving more importance to certain samples on the fly. This dynamic prioritization changes the learning target, but helps the learning process focusing on examples that have a bigger impact on how the model improves [37]. Although per-sample weighting is a key stage in dense visual prediction UDA methods to prevent the adaptation over-fit to fuzzy pseudo-label predictions [14], general per-sample adaptive weighting has not been previously explored for dense prediction visual tasks. This is probably due to the memory and computation requirements in estimating a relevance for each pixel.

To address the class-imbalance challenge in UDA, this paper describes a new algorithm-level technique: a gradient-based class-loss weighting (GBW) for UDA that can be applied to dense prediction visual tasks. GBW firstly leverages adaptive weighting for dense visual prediction tasks by considering the gradients of the per-class loss in each iteration as a proxy to the class learning and pondering the learning of the classes such that the overall loss gradient (and hence—we hypothesize, the learning) is maximized. GBW can be straightforwardly integrated into various UDA methods across different visual recognition tasks, making it highly valuable in practice. The overall effect in UDA of GBW is the alleviation of class imbalance, consistently improving the classification of low populated classes as well as the overall performance. Figure 1 shows a visual comparison of the effect of using GBW in state-of-the-art (SOTA) methods HRDA [17] for semantic segmentation and EDAPS [34] for panoptic segmentation.

Leveraging the gradient rather than class frequencies permits the application to both source and target domains, enabling its use for UDA. Performing adaptive weighting at the class rather than at the pixel level, not only effectively enables the use of adaptive weighting techniques for dense visual prediction tasks but also naturally adapts the training to each class learning landscape. This enables the learning process to evolve differently for each class based on its nature, interactions with other classes, and the training class-wise estimates (see examples of per-class weights evolution in Figure 2). Experimental evaluation reports significant and consistent performance improvements for different UDA methods (including adversarial training, entropy-minimization, and self-training) on multiple dense prediction visual tasks (semantic and panoptic segmentation), and using different network architectures (CNNs and Vision Transformers).

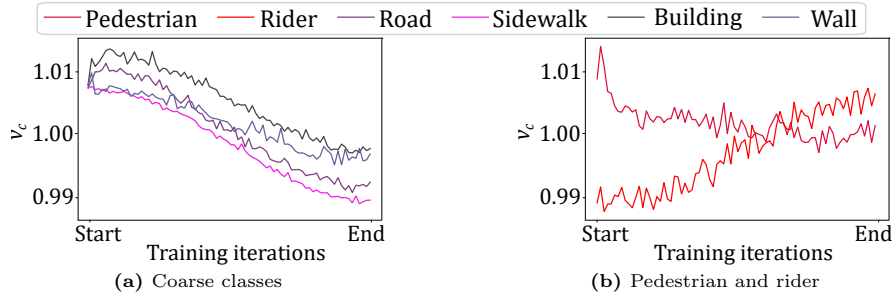


Fig. 2: Averaged per-class weights (v_c) of GBW on the GTA-Cityscapes framework for HRDA method throughout the UDA training process. **2a** shows the evolution for some coarse classes and **2b** depicts the complementary evolution for *person* and *rider*.

2 Related Work

2.1 Unsupervised Domain Adaptation: UDA

The goal of UDA is to provide robustness to co-variate shifts on an unlabeled target domain by leveraging training on a labeled source domain. Due to the universality of domain gaps, the use of UDA has been explored in multiple computer vision problems, including image classification [18, 30], semantic segmentation [16, 17] and panoptic segmentation [34].

UDA methods can be classified into three non-exclusive principal categories [39]: Input space adaptation [16–18, 28, 43], feature space adaptation [44, 47] and output space adaptation [1, 16, 44, 47]. **Input space adaptation** methods reduce the domain gap by modifying the style of images following a data transformation protocol based on data augmentations [28, 43], the mixture of images [43] or style transfer [49, 51]. These transformations can be applied to either the source or target domains. **Feature space adaptation** methods follow the hypothesis that minimizing a discrepancy metric between the source and target model outputs will produce domain-agnostic features. Thereby, a classifier capable of generalizing to both domains indistinguishably can be trained. This alignment is typically driven by adversarial training [44, 47] or by minimizing a suitable metric between features such as L2 distance [7, 16] or the Maximum Mean Discrepancy (MMD) [13, 54, 55]. **Output space adaptation** methods rely on the model’s predictions during training, often utilizing a process known as self-training, where the model adapts based on its own tentative predictions. This adaptation is typically achieved through the assignment of pseudo-labels, often under some confidence paradigm [16–18, 43]. However, as the model is expected to provide false positives, a prominent challenge raises: *concept drifting* [4, 36], which is the event where a model trained on pseudo-labels over-fits to false positives, consequently reducing the performance on the target domain.

Transversal to all these categories is the problem of class imbalance: Input space adaptation methods employ multiple versions of source images (reinforcing

the source class-biases), feature space adaptation aims to generate source agnostic features based on source-biased features, and output space adaptation employ source-biased predictions to generate pseudo-labels. Thus, all UDA stages may benefit from better techniques to handle class imbalance.

2.2 Handling class imbalance in UDA

In real-world scenarios, accurately classifying examples from an infrequent class poses a significant challenge known as the class imbalance problem. For image classification, competitive datasets, such as CIFAR-10/100 [25], ImageNet [9], Caltech-101/256 [15], and MIT-67 [31], deliberately hampers class imbalance by ensuring all classes have a minimum representation [22]. Unfortunately, this balanced-samples design becomes infeasible in the context of dense tasks such as semantic segmentation. Certain classes, regardless of the number of available images, inevitably exhibit significantly smaller representations compared to broader classes. Furthermore, for some domains it is not possible to obtain more images from certain classes, such as rare illnesses for medical tasks. Therefore, mitigating the adverse effects of imbalanced class distributions emerges as a transversal research problem [22, 29, 35].

Techniques to handle class imbalance in machine learning can be broadly classified into two main categories [20, 41]: data-level and algorithmic-level techniques. Data-level techniques try to balance the data by reducing the likelihood of selecting majority class samples for training (undersampling) or increasing the likelihood of minority class sampling (oversampling) [41]. On the other hand, algorithmic-level techniques modify the learning process to tackle the bias produced by the imbalanced data. These techniques are typically implemented with a weight schema assigning penalties to each class [20, 22, 24, 27]. Alternatively, hard class-weighting strategies have been proposed for semantic segmentation so that all classes contribute equally in the loss [42, 56, 60]. However, these strategies are not well suited for densely populated images, as result in small objects accounting equally in the loss to classes composing most of the scene.

In the context of UDA for dense tasks, data-level techniques are the default and typically the only imbalance techniques employed [16–18, 34]. This is mainly because standard data-level techniques rely on the source domain class frequency and algorithmic-based techniques are not effective without target domain class-frequency [54, 55]. Although a few works have explored algorithmic-level techniques, these either require the estimation of the target dataset class-frequency at every model update [54, 55] or are focused on relaxing the filtering criteria of pseudo-labels for low-populated classes [38, 61]. The former becomes unpractical for dense tasks, as such estimation must be performed at every model update making the process very time consuming. The latter does not tackle the root problem because, as the model is trained with the source biases, the pseudo-labels are more prone to classify least represented classes as other densely populated classes in the source set. Altogether, current state-of-the-art UDA methods for dense tasks rely solely on the employment of sampling techniques [16–18, 34],

discarding the possible benefits of joint training with data and algorithmic imbalance techniques [20, 41].

This paper describes a new algorithmic-level technique complementary with data-level techniques that can be applied to source and target domain, not requiring target domain information, by firstly tailoring adaptive weighting [37] to a class-wise paradigm and incorporating it into the UDA learning process.

3 Method

3.1 The learning of dense prediction visual tasks

Let $\hat{y}_{i,t} = G(x_i; \theta_t)$ be the output of a deep learning model parameterized by θ , at the t^{th} training step, given an input sample \mathbf{x}_i . In the context of classification, $\hat{y}_{i,t}$ is typically a per-class probability vector. Note that for dense tasks such as semantic and panoptic segmentation, a sample is considered to be a pixel from the image.

The learning is typically driven by maximizing the probability of the expected class y_i . This can be segregated on a per-class basis:

$$\mathcal{L}(\hat{y}_{i,t}, y_i) = \sum_{c=1}^C \frac{l_c(\hat{y}_{i,t}, y_i)}{|y_i = c|}, \quad (1)$$

where C is the number of classes, $L(\hat{y}_{i,t}, y_i)$ is the aggregated loss, l_c the probability distance of the prediction to a given class and $|\cdot|$ the cardinal function. For source domain labels and target domain pseudo-labels, l_c is typically the cross-entropy loss: $l_c(\hat{y}_{i,t}, y_i) = -\delta[c - y_i] \log(\hat{y}_{i,t})$. Furthermore, for the target domain some regimes also minimize the entropy of the predictions [47]: $l_c(\hat{y}_{i,t}) = -\hat{y}_{i,t}^c \log(\hat{y}_{i,t}^c)$.

Including into the formulation a set of per-class weights $\mathbf{v} \in \mathbb{R}^C$, the loss for each sample is defined by:

$$\mathcal{L}(\hat{y}_{i,t}, y_i; \mathbf{v}) = \sum_{c=1}^C v_c \frac{l_c(\hat{y}_{i,t}, y_i)}{|y_i = c|}. \quad (2)$$

When no class weighting is applied \mathbf{v} is a vector of one value elements of size C .

The learning of θ is driven by the minimization of the loss \mathcal{L} over N samples:

$$\theta^* = \arg \min_{\theta} \frac{1}{N} \sum_{i=1}^N \mathcal{L}(\hat{y}_{i,t}, y_i). \quad (3)$$

This optimization is often solved through stochastic gradient descent (SGD) with mini-batches, leading to the update equation:

$$\theta_{t+1} = \theta_t - \eta \frac{1}{M} \sum_{i=1}^M \nabla_{\theta_t} \mathcal{L}(\hat{y}_{i,t}, y_i; \mathbf{v}_t), \quad (4)$$

where η represents the learning rate, t the optimization step, and the samples $i = 1, \dots, M$ are selected randomly from the training set.

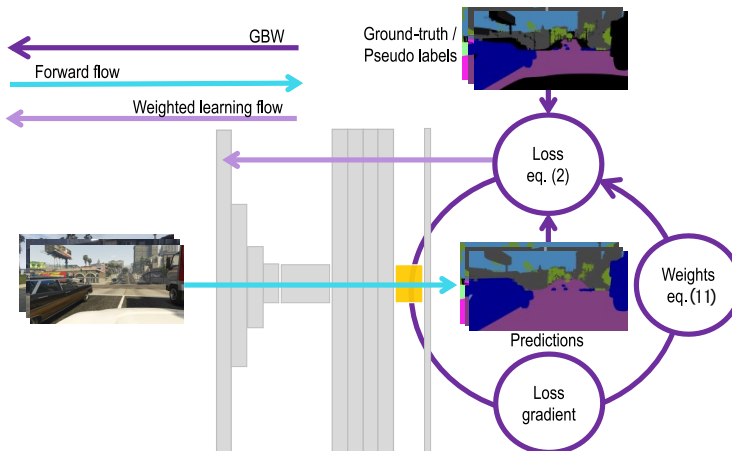


Fig. 3: Semantic segmentation using GBW. Given a forward pass of an image and the respective per-class loss (l_c). First, the gradients ($\|\nabla_{\theta_t} \bar{l}_c\|^2$) are estimated with the gradient of the last layer (shadowed in orange) to compute the per-class weights \mathbf{v} . Second, the backward pass is performed *wrt* the weighted cross entropy $\mathcal{L}(\hat{\mathbf{y}}_{i,t}, y_i; \mathbf{v}_t)$.

3.2 Gradient based weighting (GBW)

We adapt [37] by following the assumption that minimizing a class loss should make the model more prone to classify that class, therefore, by dynamically setting optimal weights to decrease the overall gradient, the model should avoid over-fitting to broad classes. Additionally, this avoids manually setting class weights which could lead to over-classifying small classes. To that end, GBW estimates class weights at each learning step given the average per-class loss (\bar{l}_c) gradients:

$$\mathbf{v}^* = \arg \min_{\mathbf{v}} \bar{l}_c(\hat{\mathbf{y}}_{i,(t+1)}, y_i; \mathbf{v}_t) - \bar{l}_c(\hat{\mathbf{y}}_{i,t}, y_i; \mathbf{v}_t). \quad (5)$$

Using linear approximation, one can approximate the term $\bar{l}_c(\hat{\mathbf{y}}_{i,(t+1)}, y_i; \mathbf{v}_t)$:

$$\bar{l}_c(\hat{\mathbf{y}}_{t+1}, y_i; \mathbf{v}_t) \leq \{\bar{l}_c(\hat{\mathbf{y}}_{i,t}, y_i; \mathbf{v}_t) + (\nabla_{\theta_t} \bar{l}_c(\hat{\mathbf{y}}_{i,t}, y_i; \mathbf{v}_t))^T (\theta_{t+1} - \theta_t)\} \quad (6)$$

Note that $\nabla_{\theta_t} \bar{l}_c(\cdot; \mathbf{v}_t) = \frac{1}{C} \sum_{c=1}^C v_c \nabla_{\theta_t} l_c$, making the operation linearly dependant on the per-class losses.

$$\begin{aligned} & \bar{l}_c(\hat{\mathbf{y}}_{i,t}, y_i; \mathbf{v}_t) - \bar{l}_c(\hat{\mathbf{y}}_{i,(t+1)}, y_i; \mathbf{v}_t) \\ & \text{including Eq 6} \\ & \leq \bar{l}_c(\hat{\mathbf{y}}_{i,t}, y_i; \mathbf{v}_t) - \bar{l}_c(\hat{\mathbf{y}}_{i,t}, y_i; \mathbf{v}_t) - (\nabla_{\theta_t} \bar{l}_c(\hat{\mathbf{y}}_{i,t}, y_i; \mathbf{v}_t))^T (\theta_{t+1} - \theta_t) \\ & = -(\nabla_{\theta_t} \bar{l}_c(\hat{\mathbf{y}}_{i,t}, y_i; \mathbf{v}_t))^T (\theta_{t+1} - \theta_t) \\ & \text{including Eq 4 and simplifying} \\ & = (\nabla_{\theta_t} \bar{l}_c(\hat{\mathbf{y}}_{i,t}, y_i; \mathbf{v}_t))^T (\eta \nabla_{\theta_t} \bar{l}_c(\hat{\mathbf{y}}_{i,t}, y_i; \mathbf{v}_t)) \\ & = \eta \|\nabla_{\theta_t} \bar{l}_c(\hat{\mathbf{y}}_{i,t}, y_i; \mathbf{v}_t)\|^2. \end{aligned} \quad (7)$$

Class weights can be calculated through the following optimization problem:

$$\begin{aligned} \mathbf{v}^* = \arg \min_{\mathbf{v}} & -\|\nabla_{\theta_t} \bar{l}_c(\hat{\mathbf{y}}_{i,t}, y_i; \mathbf{v}_t)\|^2 \\ & \text{subject to } v_c \geq 0, \forall c \in [1, C] \end{aligned} \quad (8)$$

This optimization can be efficiently computed by expressing the problem as a quadratic programming problem [45]:

$$\begin{aligned} \text{minimize } & \mathbf{v}_t^T Q \mathbf{v}_t - (\|\nabla_{\theta_t} \bar{l}_c\|^2)^T \mathbf{v}_t \\ & \text{subject to } -I \mathbf{v}_t \leq \mathbf{0}, \end{aligned} \quad (9)$$

where $\mathbf{0}$ is a vector filled with zeros and I is the identity matrix. The only problem left is defining the Q matrix. Through initial experimentation, we found that this optimization would lead to highly variable weights which disrupt learning. Therefore, we opt to define Q as a regularization matrix: $Q = \lambda I$, where λ is a regularization parameter. Specifically, we impose an L_2 regularization on \mathbf{v}_t :

$$\begin{aligned} \mathbf{v}^* = \arg \min_{\mathbf{v}} & -(\|\nabla_{\theta_t} \bar{l}_c\|^2)^T \mathbf{v}_t + \lambda \|\mathbf{v}_t\|^2 \\ & \text{subject to } v_c \geq 0, \forall c \in [1, C] \end{aligned} \quad (10)$$

Additionally, to maintain a similar scale to the original loss, we impose an additional constraint that ensures the weights sum up to the number of classes.

$$\begin{aligned} \mathbf{v}^* = \arg \min_{\mathbf{v}} & -(\|\nabla_{\theta_t} \bar{l}_c\|^2)^T \mathbf{v}_t + \lambda \|\mathbf{v}_t\|^2 \\ & \text{subject to } v_c \geq 0, \forall c \in [1, C] \\ & \text{and } \sum_{c=1}^C v_c = C, \end{aligned} \quad (11)$$

the last constraint also promotes that all batches are weighted similarly in the loss, as without it, we seldom noticed large discrepancies for some instances and training iterations that were precluding a smooth learning process.

Overall, the complexity of GBW scales with the number of classes: $O(C)^2$, making its resolution feasible for large datasets. However, to further facilitate the computation of the gradient norms without performing back-propagation throughout the entire model, the gradient norms are further approximated by calculating the gradient of the loss function with respect to the pre-activation outputs of the last layer in the model. The use of these pre-activation gradients, as demonstrated in previous studies [21, 37], significantly simplifies the weight computation process and substantially reduces computational complexity, while preserving a significant correlation to the true gradients. Figure 3 provides a visual summary of our GBW methodology for semantic segmentation.

Combination with previous per-sample weighting In UDA, pseudo-labels are commonly employed to reinforce the classification performance on the target data. These pseudo-labels usually are weighted at a sample level to avoid over-fitting to fuzzy predictions [14, 16–18, 26, 40, 43, 50]. Notably, neglecting these pseudo-labels in the optimization goal leads to the class-weights counteracting the confidence weighting in the loss. To prevent this, we modify the optimization goal in Equation 11 by incorporating the pseudo-label confidence p_i :

$$\mathbf{v}^* = \arg \min_{\mathbf{v}} -(\|\nabla_{\theta_t} \sum_{i=1}^M p_i \cdot l_c(\hat{\mathbf{y}}_{i,t}, y_i)\|^2)^T + \lambda \|\mathbf{v}_t\|^2. \quad (12)$$

4 Experimental Exploration

4.1 Setup

Semantic Segmentation We explore the benefits of the proposed GBW method on two popular UDA scenarios defined by the adaptation for semantic segmentation of the source datasets GTA [32] and Synthia [33] to the target dataset Cityscapes [8]. **GTA** is a synthetic dataset comprising 25K images and sharing 19 semantic classes with Cityscapes. **Synthia** is a synthetic urban scenes dataset for semantic segmentation, composed of 9.5K images and with 16 common semantic classes with Cityscapes. **Cityscapes** is a real-image dataset with urban scenes generated by filming with a camera inside of a car while driving through different German cities. It consists of 3K images for training and 0.5K images for validation. For evaluation, we rely on the common metric used for semantic segmentation: the per-class intersection over union (IoU) [11], between the model prediction and the ground-truth label. IoU measures at pixel-level the relationship between True Positives (TP), False Positives (FP) and False Negatives (FN): $IoU = \frac{TP}{TP+FP+FN}$.

Panoptic Segmentation Similarly to Semantic segmentation, we measure the benefits of GBW for UDA between the synthetic source dataset Synthia [33] and the real target dataset Cityscapes [8]. These are evaluated through common Panoptic segmentation metrics: mean Segmentation Quality (mSQ), mean Recognition Quality (mRQ) and mean Panoptic Quality (mPQ) [23]. The mSQ measures the closeness of the predicted segments with their ground truths, mRQ is equivalent to the F1 score and the mPQ presents a global quality of the panoptic segmentation by combining at a per-class level the SQ and RQ: $PQ = SQ \times RQ$. Note that improving the recall of an algorithm mainly affects mRQ, as mSQ is mostly driven by the segmentation quality of the TP [23].

Training parameters The architectures employed and all training parameters but our proposed weight regularization in equation 11, are as in the original papers [16–18, 34, 43, 44, 47].

Architecture	UDA Method	data-level	GTA		Synthia	
			w/o GBW	w/ GBW	w/o GBW	w/ GBW
Convolutional	Output [47]	×	43.8	46.1	38.1	41.2
	Feature [44]	×	42.4	45.5	46.7*	50.7*
	Input [43]	×	52.1	55.4	48.3	50.1
Transformer	Output + Input [16]	✓	68.3	69.2	60.9	62.3
	Output + Input [17]	✓	73.8	74.7	65.8	66.8
	Output + Input [18]	✓	75.9	76.4	67.5	68.8

Table 1: Comparison of UDA methods for the GTA-Cityscapes and Synthia-Cityscapes semantic segmentation frameworks for different architectures and methods.

4.2 GBW for UDA in Semantic Segmentation

Incorporation of GBW into UDA methods Table 1 measures the performance gain of key state-of-the-art UDA methods in the GTA-Cityscapes and Synthia-Cityscapes scenarios when GBW is incorporated. Methods are arranged according to the use (marked with a ✓) or not (marked with a ×) of some form of data-level class imbalance techniques. The results show that incorporating our per-class weighting strategy consistently leads to performance gains across various architectures and methods. Notably, the largest gains are observed for methods that do not employ data-level class imbalance techniques, with improvements of up to 3.3 points in mIoU for GTA-Cityscapes and 4.0 for Synthia-Cityscapes. GBW provides moderate gains also for methods that already utilize data-level class imbalance techniques, underlining its complementary nature to these strategies.

Architecture	Method	GTA-Cityscapes	Synthia-Cityscapes
Convolutional	CRA [50]	46.7	49.3
	Zhang et al. [58]	48.2	48.4
	GBW (DACS)	55.4	50.1
Transformer	ExpCons [48]	69.6	61.5
	DiGA [40]	70.0	62.1
	MIC [18]	75.9	67.5
	GBW (MIC)	76.4	68.8

Table 2: Comparison of leading GTA-Cityscapes and Synthia-Cityscapes UDA semantic segmentation frameworks for convolutional- and transformer-based architectures.

Comparison with state-of-the-art Table 2 provides a comprehensive comparison of the currently state-of-the-art convolutional-based and transformer-based models. Notably, the inclusion of GBW in the learning of MIC [18] results in performance gains compared to the other analysed state-of-the-art methods for both scenarios. Importantly, GBW achieves these results without the need for computationally expensive transformations such as style transfer [50], or feature prototyping [28, 58].

4.3 GBW for UDA in Panoptic segmentation

For panoptic segmentation UDA, we explore the benefits of including GBW in the learning process of the state-of-the-art method EDAPS [34]. In the Synthia-

Method	mPQ	mSQ	mRQ
CVRN [19]	32.1	66.6	40.9
UniDAPS [59]	33.0	64.7	42.2
EDAPS [34]	41.2	72.7	53.6
GBW (EDAPS)	43.0	73.2	55.9

Table 3: Performance comparison of state-of-the-art Synthia-Cityscapes UDA panoptic segmentation frameworks. Best results indicated in bold.

Cityscapes scenario (Tab. 3), the use of GBW provides improvements across all metrics. Specifically of +0.5 mSQ, +1.8 mPQ and +2.3 mRQ. As mSQ measures the segmentation quality of the true positives, it is mostly driven by the segmentation capabilities of the network, thus, the gain in terms of mSQ is narrower. To the best of our knowledge, this GBW-enhanced EDAPS setup is the current state-of-the-art for UDA in panoptic segmentation across all metrics.

4.4 Analysis of GBW

Combination with data-level class imbalance techniques Currently, the default technique for handling class imbalance in UDA is rare class sampling [16]. Therefore, we propose to analyze the impact of GBW when used in conjunction and separated from the standard data-level technique. Table 4a presents a comparison of various configurations incorporating per-class weights and class-uniform sampling. The results emphasize the substantial impact of these techniques in the performance of the DAFormer method for semantic segmentation UDA [16]: the combined approach yields +7.5 points increase in terms of mIoU.

	None	w/GBW	w/S	w/GBW+S	Loss	wo	w/IF	w/PF	w/LBW	w/GBW
mIoU	61.7	65.2	68.3	69.2	CE	73.8	71.3	30.7	72.9	74.7
Gain	0	3.5	6.6	7.5	FL [27]	68.9	68.5	64.0	68.9	70.1

(a) Data-level techniques on DAFormer [16].

(b) Algorithmic-level techniques on HRDA [17].

Table 4: Performance comparison with alternative data and algorithmic level class imbalance techniques on the GTA-Cityscapes semantic segmentation framework [16]. Key:S: Sampling. CE: Cross-entropy. FL: Focal-loss. IF: image frequency. PF: pixel frequency. LBW: loss-based weighting.

Effect on different segmentation losses Table 4b compiles the performances of incorporating in the learning process state-of-the-art class weighting strategies, including regular class weights [46]: the inverse frequency on the source set, either considering the pixel-level frequency (PF) [3] or the image-level frequency (IF) [6], and a class weighting based on the per class loss rather than their gradient (LBW) [10]. Reported performance corroborate the previous evidence that weighting the loss based on source domain priors do not transfer well to the target domain due to the distribution shift. Regarding the frequency source, PF results in drastically higher weights for underrepresented classes compared to IF, turning the model prone to classify broad structures as low-represented categories, thus presenting a significant drop in performance. Meanwhile, IF

weighting assigns more uniform weights, thus, presenting better performance than PF, but dropping the performance of broad categories compared to GBW. The use of LBW results in second performance, but suffers from a stable tendency that prevents it from quickly adapting to the learning outcomes as GBW.

Per-class improvements Figure 4a, depicts the disparity between the state-of-the-art model HRDA confusion matrix [17] and the confusion matrix of the modified HRDA after the inclusion of GBW. Introducing GBW notably enhances recall, as evidenced by the predominantly positive values along the diagonal (15 out of 19). Note that the gain in recall is specially significant for the least represented classes in the source dataset (GTA): *train*, *motorcycle* and *bicycle*. This is evidenced by the true positives on the diagonal. Although GBW-enhanced model shows improvements for most classes, it is observed that some classes as *sidewalk* and *motorcycle* do not benefit from it. This is further analyzed in the Supplementary material.

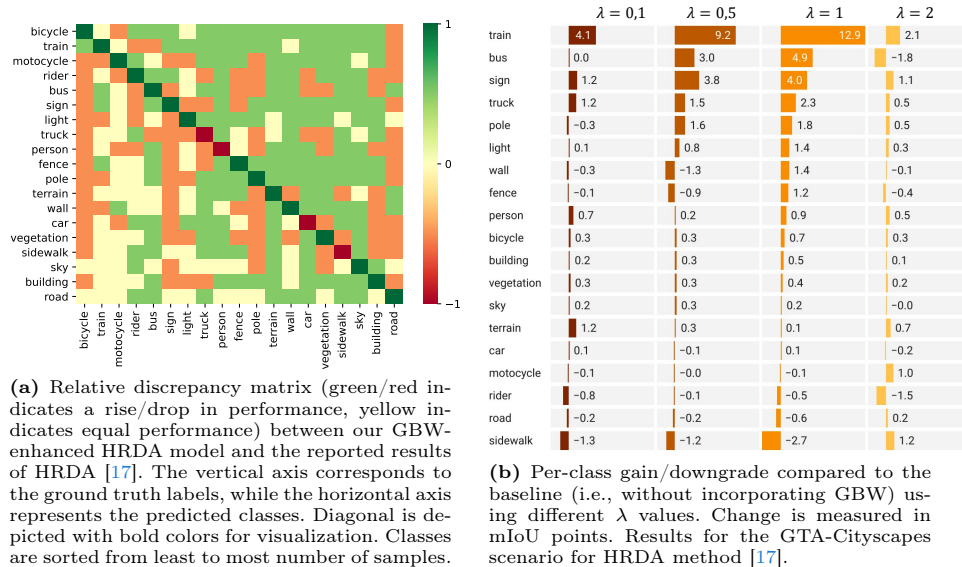


Fig. 4: GBW per-class performance analysis.

Figure 5 includes a qualitative comparison between models trained with and without GBW. The GBW-model exhibits enhanced capability in accurately classifying less populated classes. See examples for *fence* (second row), *bus* and *sign* (fourth row). See Supplementary material for more visual examples.

Regularization weight This section examines the impact of the regularization factor when GBW is incorporated into the HRDA model [17] for semantic segmentation, as shown in Table 5. Note that λ represents the weight of the regularization term in Equation 11, with higher values enforcing uniform weights, which is equivalent to not applying any weighting at all. This is clearly observed in the

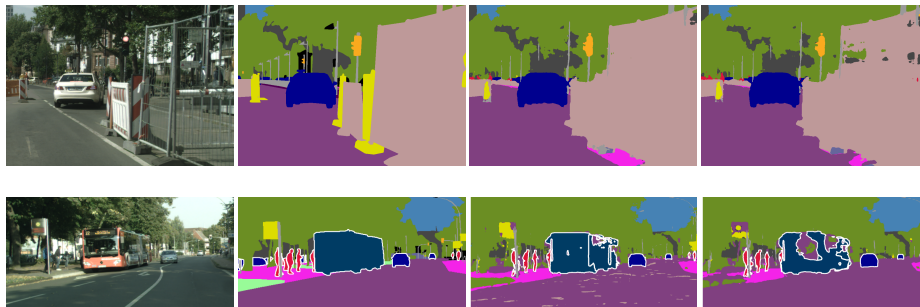


Fig. 5: Qualitative comparison. Column-wise: image, ground truth, model trained with and without GBW. Semantic segmentation (1st row). Panoptic segmentation (2nd row).

performance when $\lambda = 10$, which matches the performance of a model trained without GBW. Conversely, extremely small λ values may cause the weights of certain classes approach to zero, effectively disregarding them during training. This accounts for the suboptimal performance observed when $\lambda = 0.01$. Figure 4b visualize disentangles this effect in per-class performance. GBW drastically affects *train* and visually similar classes (*bus*, *truck*) performance, with improvements of over +10 IoU. We believe this to be because *train* is the second least represented class in the GTA [32] dataset and models trained on GTA tend to classify it as *bus* and *truck*, thus improving also their IoU by reducing FPs.

λ	-	0.01	0.1	0.5	1	2	10
mIoU	73.2	56	73.5	73.8	74.7	73.8	73.2
Gain	-	-16.8	0.3	0.6	1.5	0.6	0.0

Table 5: Ablation study for the λ weight on the GTA-Cityscapes framework embedded into the state-of-the-art UDA method HRDA [17]

Weight distribution The main hypothesis is that a GBW-enhanced model tends to promote the learning of under-represented classes. To visually inspect this, Figure 6a compares the percentage of pixels per class in the source dataset with the maximum weight assigned by GBW, showcasing that highly represented classes tend to be given a smaller weight than less represented classes. The Figure only depicts the maximum weight per class along the training, as weights are made to be very variable between training iterations depending on the current state of the model. It can be observed that classes that presented a large variation in weights, such as *train* and *sign*, are associated with larger improvements in performance, with increases of over 12 points in mIoU. Figure 6b illustrates the relationship between weight variance and mIoU. Note how classes with performance improvements highly correlate with the variability of the assigned weights. Additionally, highly represented classes as *road* and *sidewalk*, exhibit more uniform weights, indicated by a low standard deviation.

Weight evolution Figures 2a and 2b present the averaged evolution of the per-class weights assigned by GBW. Coarse and high populated classes (as shown in

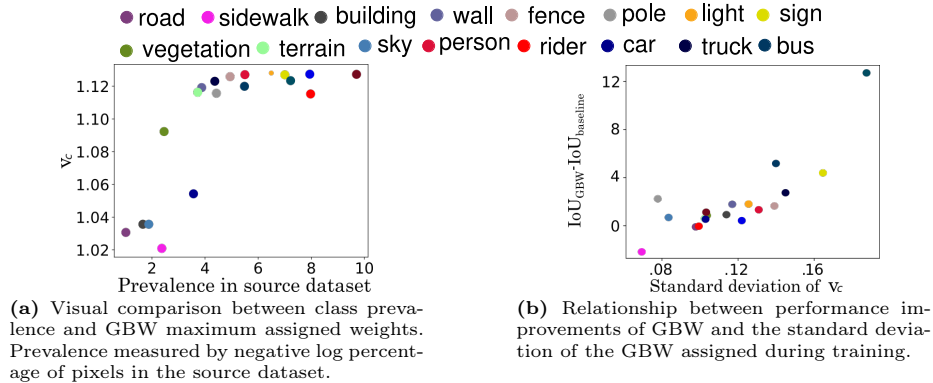


Fig. 6: Analysis of the GBW weights assigned throughout the training with HRDA [17].

Figure 2a) start the training process with higher weights. However, as training progresses, these weights gradually decrease and are distributed to other classes. Specifically, looking at two similar classes: *person* (highly populated) and *rider* (under-populated) GBW adeptly handles them by assigning higher weights to *person* at the onset of training, while lowering the weight for *rider* (see Figure 2b). As the training proceeds, the weight assigned to *rider* gradually increases, while decreasing simultaneously the weight for *person* suggesting an interesting capacity of GBW in adapting to the training outcomes. This, together with previous evidences, suggests that the success of GBW relies on the algorithm’s capacity to dynamically assign appropriate weights to each class at different stages of the learning process naturally and dynamically integrating evidences from all classes.

5 Conclusion

Despite the extensive literature in UDA, the impact of statistical discrepancies—such as different class imbalances between the source and target dataset—is still an open topic. Due to the lack of target labels, algorithmic-level techniques to handle class imbalance are deemed unsuited for UDA in dense prediction visual tasks. In this work, class imbalance is handled by an adaptive weighting scheme based on the loss gradients at each training step. Per-class weights are updated on-the-fly at each training step to compensate for the magnitudes of the loss gradient. Experimental results show improvements in the recall of scarcely represented classes. The benefits of GBW are exhaustively explored by means of its introduction into six different state-of-the-art UDA methods for semantic segmentation and panoptic segmentation. The results consistently show that incorporating GBW leads to performance gains across different architectures and datasets for both semantic and panoptic segmentation. We hope that GBW can be used on future UDA methods by serving as a building block for narrowing the gap between UDA and supervised methods.

References

1. A.K., D., Sanodiya, R.K., Jose, B.R., Mathew, J.: Visual domain adaptation through locality information. *Engineering Applications of Artificial Intelligence* **123**, 106172 (2023). <https://doi.org/https://doi.org/10.1016/j.engappai.2023.106172> 4
2. Alcover-Couso, R., Escudero-Vinolo, M., SanMiguel, J.C., Martinez, J.M.: Soft labelling for semantic segmentation: Bringing coherence to label down-sampling (2023) 2
3. Alonso, I., Sabater, A., Ferstl, D., Montesano, L., Murillo, A.C.: Semi-supervised semantic segmentation with pixel-level contrastive learning from a class-wise memory bank. In: *IEEE Conf. Comput. Vis. Pattern Recognit. (CVPR)* (2021) 11
4. Cascante-Bonilla, P., Tan, F., Qi, Y., Ordonez, V.: Curriculum labeling: Revisiting pseudo-labeling for semi-supervised learning. In: *AAAI Conference on Artificial Intelligence* (2020) 4
5. Chen, J., Yang, Z., Zhang, L.: Semantic segment anything (2023) 2
6. Chen, M., Xue, H., Cai, D.: Domain adaptation for semantic segmentation with maximum squares loss. In: *IEEE Int. Conf. Comput. Vis. (ICCV)*. pp. 2090–2099 (October 2019). <https://doi.org/10.1109/ICCV.2019.00218> 11
7. Chen, Y., Li, W., Van Gool, L.: Road: Reality oriented adaptation for semantic segmentation of urban scenes. In: *IEEE Conf. Comput. Vis. Pattern Recognit. (CVPR)* (2017) 4
8. Cordts, M., Omran, M., Ramos, S., Rehfeld, T., Enzweiler, M., Benenson, R., Franke, U., Roth, S., Schiele, B.: The cityscapes dataset for semantic urban scene understanding. In: *IEEE Conf. Comput. Vis. Pattern Recognit. (CVPR)*. pp. 3212–3223 (2016). <https://doi.org/10.1109/CVPR.2016.350> 2, 9
9. Deng, J., Dong, W., Socher, R., Li, L.J., Li, K., Fei-Fei, L.: Imagenet: A large-scale hierarchical image database. In: *IEEE Conf. Comput. Vis. Pattern Recognit. (CVPR)*. pp. 248–255 (2009). <https://doi.org/10.1109/CVPR.2009.5206848> 5
10. Escudero-Viñolo, M., López-Cifuentes, A.: Ccl: Class-wise curriculum learning for class imbalance problems. In: *2022 IEEE Int. Conf. Image Process. (ICIP)*. pp. 1476–1480 (2022). <https://doi.org/10.1109/ICIP46576.2022.9897273> 11
11. Everingham, M., Gool, L.V., Williams, C.K.I., Winn, J., Zisserman, A.: The pascal visual object classes (voc) challenge (2010) 9
12. Fernández-Moreno, M., Lei, B., Holm, E.A., Mesejo, P., Moreno, R.: Exploring the trade-off between performance and annotation complexity in semantic segmentation. *Engineering Applications of Artificial Intelligence* **123**, 106299 (2023). <https://doi.org/https://doi.org/10.1016/j.engappai.2023.106299> 2
13. Gao, L., Zhang, J., Zhang, L., Tao, D.: Dsp: Dual soft-paste for unsupervised domain adaptive semantic segmentation. In: *ACM Int. Conf. Multimedia (MM)*. p. 2825–2833 (2021). <https://doi.org/10.1145/3474085.3475186> 4
14. Gong, R., Wang, Q., Danelljan, M., Dai, D., Van Gool, L.: Continuous pseudo-label rectified domain adaptive semantic segmentation with implicit neural representations. In: *IEEE Conf. Comput. Vis. Pattern Recognit. (CVPR)*. pp. 7225–7235 (June 2023) 3, 9
15. Griffin, G., Holub, A., Perona, P.: Caltech 256 (2022). <https://doi.org/10.22002/D1.20087> 5
16. Hoyer, L., Dai, D., Van Gool, L.: DAFormer: Improving network architectures and training strategies for domain-adaptive semantic segmentation. In: *IEEE Conf. Comput. Vis. Pattern Recognit. (CVPR)*. pp. 9924–9935 (2022) 2, 4, 5, 9, 10, 11

17. Hoyer, L., Dai, D., Van Gool, L.: HRDA: Context-aware high-resolution domain-adaptive semantic segmentation. In: IEEE Eur. Conf. Comput. Vis. (ECCV). p. 372–391 (2022) [2](#), [3](#), [4](#), [5](#), [9](#), [10](#), [11](#), [12](#), [13](#), [14](#)
18. Hoyer, L., Dai, D., Wang, H., Van Gool, L.: MIC: Masked image consistency for context-enhanced domain adaptation. In: IEEE Conf. Comput. Vis. Pattern Recognit. (CVPR) (2023) [2](#), [4](#), [5](#), [9](#), [10](#)
19. Huang, J., Guan, D., Xiao, A., Lu, S.: Cross-view regularization for domain adaptive panoptic segmentation. In: IEEE Conf. Comput. Vis. Pattern Recognit. (CVPR) (2021) [11](#)
20. Johnson, J.M., Khoshgoftaar, T.M.: Survey on deep learning with class imbalance. In: Journal of Big Data (2019). <https://doi.org/10.1186/s40537-019-0192-5> [2](#), [5](#), [6](#)
21. Katharopoulos, A., Fleuret, F.: Not all samples are created equal: Deep learning with importance sampling. In: International Conference on Machine Learning (2018) [3](#), [8](#)
22. Khan, S.H., Hayat, M., Bennamoun, M., Sohel, F.A., Togneri, R.: Cost-sensitive learning of deep feature representations from imbalanced data. IEEE Transactions on Neural Networks and Learning Systems **29**(8), 3573–3587 (2018). <https://doi.org/10.1109/TNNLS.2017.2732482> [2](#), [3](#), [5](#)
23. Kirillov, A., He, K., Girshick, R., Rother, C., Dollar, P.: Panoptic segmentation. In: IEEE Conf. Comput. Vis. Pattern Recognit. (CVPR) (2019) [9](#)
24. Krawczyk, B.: Learning from imbalanced data: open challenges and future directions. In: Progress in Artificial Intelligence (2016). <https://doi.org/10.1007/s13748-016-0094-0> [5](#)
25. Krizhevsky, A., Nair, V., Hinton, G.: Cifar-10 (canadian institute for advanced research). Kaggle (2010) [5](#)
26. Li, T., Roy, S., Zhou, H., Lu, H., Lathuilière, S.: Contrast, stylize and adapt: Unsupervised contrastive learning framework for domain adaptive semantic segmentation. In: IEEE Conf. Comput. Vis. Pattern Recognit. (CVPR) Workshops. pp. 4868–4878 (June 2023) [9](#)
27. Lin, T.Y., Goyal, P., Girshick, R., He, K., Dollar, P.: Focal loss for dense object detection. In: IEEE Conf. Comput. Vis. (ICCV) (2017) [5](#), [11](#)
28. Nam, K.D., Nguyen, T.M., Dieu, T.V., Visani, M., Nguyen, T.O., Sang, D.V.: A novel unsupervised domain adaptation method for depth-guided semantic segmentation using coarse-to-fine alignment. IEEE Access **10**, 101248–101262 (2022). <https://doi.org/10.1109/ACCESS.2022.3205414> [4](#), [10](#)
29. Pihur, V., Datta, S., Datta, S.: Weighted rank aggregation of cluster validation measures: a monte carlo cross-entropy approach. Bioinformatics pp. 1607–1615 (2007). <https://doi.org/10.1093/bioinformatics/btm158> [5](#)
30. Qu, S., Zou, T., Röhrbein, F., Lu, C., Chen, G., Tao, D., Jiang, C.: Upcycling models under domain and category shift. In: IEEE Conf. Comput. Vis. Pattern Recognit. (CVPR) (2023) [4](#)
31. Quattoni, A., Torralba, A.: Recognizing indoor scenes. In: 2009 IEEE conference on computer vision and pattern recognition. pp. 413–420. IEEE (2009) [5](#)
32. Richter, S.R., Vineet, V., Roth, S., Koltun, V.: Playing for data: Ground truth from computer games. In: IEEE Eur. Conf. Comput. Vis. (ECCV). pp. 102–118 (2016). https://doi.org/10.1007/978-3-319-46475-6_7 [9](#), [13](#)
33. Ros, G., Sellart, L., Materzynska, J., Vazquez, D., Lopez, A.M.: The synthia dataset: A large collection of synthetic images for semantic segmentation of urban scenes. Proc. IEEE Conf. Comput. Vis. Pattern Recognit. (CVPR) pp. 3234–3243 (2016) [9](#)

34. Saha, S., Hoyer, L., Obukhov, A., Dai, D., Gool, L.V.: Edaps: Enhanced domain-adaptive panoptic segmentation. *IEEE Int. Conf. Comp. Vis. (ICCV)* (2023) [2](#), [3](#), [4](#), [5](#), [9](#), [10](#), [11](#)
35. Salehi, S.S.M., Erdogmus, D., Gholipour, A.: Tversky loss function for image segmentation using 3d fully convolutional deep networks. In: *Machine Learning in Medical Imaging*. pp. 379–387 (2017) [5](#)
36. Sammut, C., Harries, M.: Concept drift. In: *Encyclopedia of Machine Learning*. pp. 202–205 (2010). https://doi.org/10.1007/978-0-387-30164-8_153 [4](#)
37. Santiago, C., Barata, C., Sasdelli, M., Carneiro, G., Nascimento, J.C.: Low: Training deep neural networks by learning optimal sample weights. *Pattern Recognition* **110**, 107585 (2021). <https://doi.org/https://doi.org/10.1016/j.patcog.2020.107585> [3](#), [6](#), [7](#), [8](#)
38. Saporta, A., Vu, T.H., Cord, M., Pérez, P.: Esl: Entropy-guided self-supervised learning for domain adaptation in semantic segmentation. In: *IEEE Conf. Comput. Vis. Pattern Recognit. Workshop (CVPRW)* (2020) [5](#)
39. Schwonberg, M., Niemeijer, J., Termöhlen, J.A., Schäfer, J.P., Schmidt, N.M., Gottschalk, H., Fingscheidt, T.: Survey on unsupervised domain adaptation for semantic segmentation for visual perception in automated driving. *IEEE Access* **11**, 54296–54336 (2023). <https://doi.org/10.1109/ACCESS.2023.3277785> [4](#)
40. Shen, F., Gurram, A., Liu, Z., Wang, H., Knoll, A.: Diga: Distil to generalize and then adapt for domain adaptive semantic segmentation. In: *IEEE Conf. Comput. Vis. Pattern Recognit. (CVPR)*. pp. 15866–15877 (2023) [9](#), [10](#)
41. Spelmen, V.S., Porkodi, R.: A review on handling imbalanced data. In: *Int. Conf. Current Trends towards Converging Technologies (ICCTCT)*. pp. 1–11 (2018). <https://doi.org/10.1109/ICCTCT.2018.8551020> [2](#), [5](#), [6](#)
42. Sudre, C.H., Li, W., Vercauteren, T., Ourselin, S., Jorge Cardoso, M.: Generalised dice overlap as a deep learning loss function for highly unbalanced segmentations. In: *Deep Learning in Medical Image Analysis and Multimodal Learning for Clinical Decision Support* (2017) [5](#)
43. Tranheden, W., Olsson, V., Pinto, J., Svensson, L.: Dacs: Domain adaptation via cross-domain mixed sampling. *IEEE Winter Conf. App. Comp. Vis. (WACV)* pp. 1378–1388 (2020) [2](#), [4](#), [9](#), [10](#)
44. Tsai, Y.H., Hung, W.C., Schuster, S., Sohn, K., Yang, M.H., Chandraker, M.: Learning to adapt structured output space for semantic segmentation. In: *IEEE Conf. Comput. Vis. Pattern Recognit. (CVPR)*. pp. 7472–7481 (2018). <https://doi.org/10.1109/CVPR.2018.00780> [4](#), [9](#), [10](#)
45. Vavasis, S.A.: Complexity theory: quadratic programming. *Complexity Theory: Quadratic Programming*, pp. 451–454 (2009) [8](#)
46. Veropoulos, K., Campbell, C., Cristianini, N.: Controlling the sensitivity of support vector machines. *International Joint Conference Artificial Intelligence (IJCAI)* (1999) [11](#)
47. Vu, T.H., Jain, H., Bucher, M., Cord, M., Pérez, P.: Advent: Adversarial entropy minimization for domain adaptation in semantic segmentation. In: *IEEE Conf. Comput. Vis. Pattern Recognit. (CVPR)*. pp. 2512–2521 (2019). <https://doi.org/10.1109/CVPR.2019.00262> [2](#), [4](#), [6](#), [9](#), [10](#)
48. Wang, K., Donghyun, K., Feris, R., Saenko, K., Betke, M.: Exploring consistency in cross-domain transformer for domain adaptive semantic segmentation. *IEEE Int. Conf. Comp. Vis. (ICCV)* (2023) [10](#)
49. Wang, S., Zhao, X., Chen, J.: Discovering latent target subdomains for domain adaptive semantic segmentation via style clustering. *Multimedia Tools and Appli-*

- cations pp. 3234–3243 (2023). <https://doi.org/10.1007/s11042-023-15620-6> 4
50. Wang, Z., Liu, X., Suganuma, M., Okatani, T.: Unsupervised domain adaptation for semantic segmentation via cross-region alignment. *Computer Vision and Image Understanding* p. 103743 (2023). <https://doi.org/https://doi.org/10.1016/j.cviu.2023.103743> 9, 10
 51. Wu, X., Wu, Z., Lu, Y., Ju, L., Wang, S.: Style mixing and patchwise prototypical matching for one-shot unsupervised domain adaptive semantic segmentation. In: *AAAI Conf. Art. Int.* (2022) 4
 52. Xie, E., Wang, W., Yu, Z., Anandkumar, A., Álvarez, J.M., Luo, P.: Segformer: Simple and efficient design for semantic segmentation with transformers. In: *Advances in Neural Information Processing Systems (NeurIPS)* (2021) 2
 53. Xu, X., He, H., Zhang, H., Xu, Y., He, S.: Unsupervised domain adaptation via importance sampling. *IEEE Transactions on Circuits and Systems for Video Technology* **30**(12), 4688–4699 (2020). <https://doi.org/10.1109/TCSVT.2019.2963318> 3
 54. Yan, H., Ding, Y., Li, P., Wang, Q., Xu, Y., Zuo, W.: Mind the class weight bias: Weighted maximum mean discrepancy for unsupervised domain adaptation. In: *IEEE Conf. Comput. Vis. Pattern Recognit. (CVPR)*. pp. 945–954 (2017). <https://doi.org/10.1109/CVPR.2017.107> 3, 4, 5
 55. Yan, H., Li, Z., Wang, Q., Li, P., Xu, Y., Zuo, W.: Weighted and class-specific maximum mean discrepancy for unsupervised domain adaptation. *IEEE Transactions on Multimedia* **PP**, 1–1 (2019). <https://doi.org/10.1109/TMM.2019.2953375> 3, 4, 5
 56. Yeung, M., Sala, E., Schönlieb, C.B., Rundo, L.: Unified focal loss: Generalising dice and cross entropy-based losses to handle class imbalanced medical image segmentation. *Computerized Medical Imaging and Graphics* p. 102026 (2022). <https://doi.org/https://doi.org/10.1016/j.compmedimag.2021.102026> 5
 57. Yuan, Y., Chen, X., Wang, J.: Object-contextual representations for semantic segmentation. In: *IEEE Eur. Conf. Comput. Vis. (ECCV)*. pp. 173–190 (2020) 2
 58. Zhang, J., Huang, J., Jiang, X., Lu, S.: Black-box unsupervised domain adaptation with bi-directional atkinson-shiffrin memory. *IEEE Int. Conf. Comp. Vis. (ICCV)* (2023) 10
 59. Zhang, J., Huang, J., Zhang, X., Lu, S.: Unidaformer: Unified domain adaptive panoptic segmentation transformer via hierarchical mask calibration. In: *IEEE Conf. Comput. Vis. Pattern Recognit. (CVPR)*. pp. 11227–11237 (2023). <https://doi.org/10.1109/CVPR52729.2023.01080> 11
 60. Zhao, R., Qian, B., Zhang, X., Li, Y., Wei, R., Liu, Y., Pan, Y.: Rethinking dice loss for medical image segmentation. In: *IEEE Int. Conf. on Data Mining (ICDM)*. pp. 851–860 (2020). <https://doi.org/10.1109/ICDM50108.2020.00094> 5
 61. Zou, Y., Yu, Z., Kumar, B.V., Wang, J.: Unsupervised domain adaptation for semantic segmentation via class-balanced self-training. In: *IEEE Eur. Conf. Comput. Vis. (ECCV)* (2018) 5